Investigation of charge yields, charge correlations, and multifragmentation of ^{197}Au and ^{208}Pb projectiles at beam energies between 1.0 and 158 GeV/nucleon

G. Hüntrup, T. Streibel, and W. Heinrich
Department of Physics, University of Siegen, D-57068 Siegen, Germany
(Received 6 August 1999; published 16 February 2000)

We have studied fragmentation processes of ^{208}Pb projectiles at 1.0 and 158 GeV/nucleon and of ^{197}Au projectiles at 10.6 GeV/nucleon in collisions with targets ranging from CH_2 to Pb. This is the first time projectile fragmentation has been investigated in such a large projectile energy range with the same experimental technique and with high statistical significance. For our experiments we used stacks of thin CR-39 and BP-1 nuclear track detectors. This experimental method allows measurement of the trajectories and charges of all particles with charge numbers $Z \geqslant 6$ or $Z \geqslant 7$ depending on the detection threshold. Yield spectra for the fragment charge Z and the charge sum of the detected fragments show significant target and energy dependences, which originate from different excitation energy spectra of the projectile residues in collision with light target nuclei, especially for the hydrogen target, and additionally from contributions by electromagnetic dissociation in collisions with heavy target nuclei at high beam energies. The characteristics of the breakup of the prefragment in a multifragmentation reaction were investigated based on charge correlations. No significant target dependence was observed for the different energies. This shows that the memory in the special entrance channel of the reaction is lost before the excited prefragment breaks up into smaller particles.

PACS number(s): 25.75.−q, 25.70.Mn, 25.70.Pq, 05.70.−a

I. INTRODUCTION

In the last few years the multifragmentation process has been intensively investigated in collisions of heavy projectiles with different targets in a wide spectrum of projectile energies. This decay process is of special interest due to the suggestion that multifragmentation is connected to a liquid-gas phase transition in nuclear matter [1–4]. The process of multifragmentation of excited projectile spectators produced in collisions of heavy ions with different targets has been studied at relativistic energy using different experimental techniques like electronic detector systems, emulsions, and plastic nuclear track detectors.

With electronic detector systems it is possible to measure all charged particles. These experiments can be performed with high statistical significance. Until now experiments using electronic detector systems have been carried out at projectile energies $E_P \leqslant 1.0$ GeV/nucleon. Target and projectile energy dependences of the fragmentation processes of especially heavy projectiles have been examined. It has been shown that charge correlations of fragments produced in the interactions are independent of the targets and of the projectile energy for energies between 0.4 and 1.0 GeV/nucleon [5–9].

Experiments using emulsion detectors have been performed at all available projectile energies. With this experimental technique it is also possible to measure all charged particles. However, these experiments suffer from low statistical significance because the analysis is very time consuming. Furthermore, one has to consider that emulsions are a mixture of light and heavy elements. Therefore an investigation of target dependences is difficult. On the other hand, until now the emulsion experiments are the only ones that have examined the multifragmentation process at projectile energies $E_p > 1.0$ GeV/nucleon. The results reveal a weak projectile energy dependence for some charge correlations [10–13].

We have performed experiments using the plastic nuclear track detector CR-39 at energies $E_p \leqslant 1.0$ GeV/nucleon. This experimental method allows measurement of the trajectories and charges of all relativistic particles above a charge threshold Z_t. Thus all particles with charge numbers $Z \geqslant 6$ (or $Z \geqslant 7$, depending on the sensitivity of the batch of detectors) can be analyzed [14,15]. In one of these experiments a target dependence has been observed [15], which is in contradiction to the results of experiments using electronic detector devices [9].

We have extended our investigations to higher projectile energies with an improved computerized reconstruction procedure for the interactions. Furthermore, a new experiment at 1.0 GeV/nucleon was performed to compare these results with older ones of our own group and with those of other groups using different experimental techniques as described above. Thus for the first time the target and energy dependences of fragmentation processes of heavy projectiles were investigated in reactions with different targets in a projectile energy range from 1.0 to 158 GeV/nucleon with the same experimental technique and high statistical significance. The conditions of the different experiments are summarized in Table I.

II. EXPERIMENTAL METHOD

For our experiments we used foils of the plastic nuclear track detector CR-39 with a thickness of 0.6 mm and an area between 8 cm×8 cm and 15 cm×15 cm. Our experimental setup consists of single CR-39 foils upstream from a thick target, which is called the projectile detector (Fig. 1). This allows us to identify the charges and trajectories of the incoming projectiles. Downstream from the target the fragment detector is used to measure the charges and trajectories of the projectile fragments produced in the target. The fragment detector consists of a few modules containing some CR-39 foils. Gaps between adjacent modules allow separation of

TABLE I. Summary of the analyzed experiments.

Projectile	Energy (GeV/nucleon)	Target	Target thickness (g/cm^2)	Number of projectiles	Particle density (number/cm^2)	Accelerator
^{208}Pb	1.0	CH_2	0.881 ± 0.004	116 050	2500	GSI/SIS
^{208}Pb	1.0	C	1.716 ± 0.009	114 200	2500	GSI/SIS
^{208}Pb	1.0	Cu	1.786 ± 0.009	119 050	2500	GSI/SIS
^{208}Pb	1.0	Pb	1.539 ± 0.008	119 150	2500	GSI/SIS
^{197}Au	10.6	CH_2	0.881 ± 0.004	397 350	3000	BNL/AGS
^{197}Au	10.6	C	2.565 ± 0.013	421 200	3000	BNL/AGS
^{197}Au	10.6	Pb	6.178 ± 0.031	396 300	3000	BNL/AGS
^{208}Pb	158	CH_2	0.881 ± 0.004	303 650	1000–6000	CERN/SPS
^{208}Pb	158	C	2.565 ± 0.013	160 950	1000–6000	CERN/SPS
^{208}Pb	158	Cu	3.572 ± 0.018	155 400	1000–6000	CERN/SPS
^{208}Pb	158	Pb	6.178 ± 0.031	162 950	1000–6000	CERN/SPS

projectile fragments that are produced in the same interaction. These gaps have to be adapted to the projectile energy. For the experiments at 10.6 GeV/nucleon the experimental setup differs somewhat from the other experiments. Here we used in addition one BP-1 glass detector in front of and behind the target. This detector material has an excellent charge resolution above the charge threshold $Z_t = 74$ for the analyzed experiments. This allows us to distinguish ^{197}Au projectiles from heavy fragments using a single detector side.

The irradiation of the detector material causes latent tracks along the path of the penetrating particles. These latent tracks can be developed by etching. For the experiments at 1.0, 10.6, and 158 GeV/nucleon the CR-39 foils were etched in 6*N*NaOH for 24 h at 60 °C, for 40 h at 70 °C, and for 40 h at 70 °C, respectively. The BP-1 glass detectors were etched for 14 h in 6*N*NaOH at 70 °C. During the etching process etch pits of conical shape are formed along the particle tracks on the surface of the detectors. The size of these etch pits along the tracks increases with the ionization energy loss, e.g., for relativistic particles with their charge. The position and size of the mouth of all etch cones on all foil sides can be measured with an optical microscope system. For this purpose we use the Siegen automatic measuring system [16,17].

For the reconstruction of the particle trajectories in the stacks a precise alignment of the detector foils in the setups is necessary. This can be determined based on the tracks of projectile ions. At relativistic beam energies the heavy projectiles penetrate each stack in almost straight lines. Furthermore, the projectile trajectories are almost parallel to each other and perpendicular to the detector surfaces. So one can correlate a local pattern of projectile etch cones on the first detector side with the pattern on successive detector sides. This method allows reconstruction of the projectile trajectories of the projectiles with a spatial resolution of about 2 μm. The trajectories of the projectile fragments can then easily be found in the stack coordinate system. For these tracks a precision between 2 and 10 μm can be achieved depending on the angle between the beam axis and the direction of the fragment trajectory. This reduced position resolution for the projectile fragments is mainly caused by the limited mounting precision of the detectors in the setup along the beam axis. After the reconstruction of the particle tracks one has to correlate the track of a projectile fragment with the corresponding track of an incident projectile.

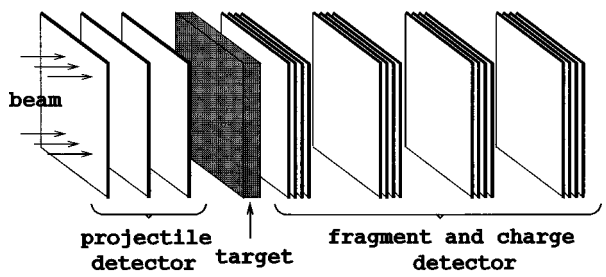

FIG. 1. Experimental setup for the experiments performed at 1.0, 10.6, and 158 GeV/nucleon.

The reconstruction of the particle tracks and vertices is performed using a computerized reconstruction procedure. The reliability of this method can be checked by a visual reconstruction of the measured etch cones [14]. Problems may arise only if the distance between two fragmenting projectiles becomes very small. To exclude ambiguities we have considered only fragmentation events where the distance to the neighboring projectile tracks on the last detector side in front of the target is larger than 50 μm.

Charge calibration of the measured particle tracks can be performed with the measured area of the etch cones. The ionization of the detector material is described by the Bethe-Bloch formula. According to this the ionization is proportional to Z^2/β^2. For the experiments at 10.6 and 158 GeV/nucleon, β is almost constant for all projectiles and projectile fragments on all detector sides. Thus the measured area of the etch cones can be related directly to the charge of the corresponding particle. For the experiments at 1.0 GeV/nucleon, however, due to the significantly different energy loss of projectiles and fragments, β depends on the depth in the stack where a fragment was produced. So it may happen that etch cones of fragments with the same measured area on the same foil side correspond to particles with a different charge and different energy. These effects were estimated using the restricted energy loss (REL_{200}) of particles in the

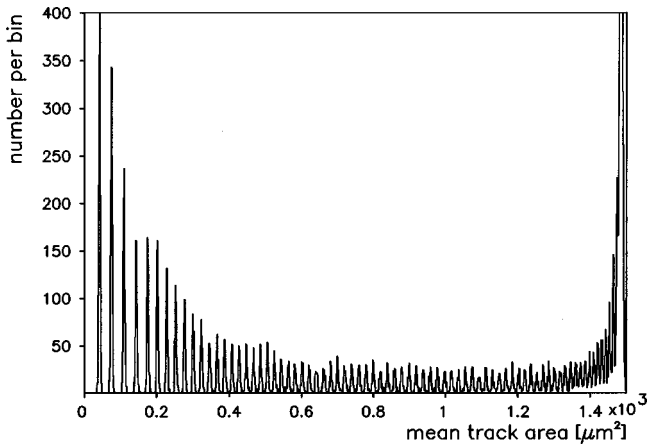

FIG. 2. Spectrum of measured mean track areas for the experiment of ^{208}Pb projectiles with a C target at 158 GeV/nucleon.

detector material [18]. This is a quantity describing the detector damage along the particle tracks in dependence on Z and β.

Furthermore, for the CR-39 detectors systematic errors may have a strong influence on the charge resolution for particles with large charge numbers. For example, it was observed that the mean measured area of the etch pits differs from foil side to foil side. This is caused by somewhat different conditions during the measuring procedure. Fortunately, these systematic deviations can be corrected for [19]. The spectrum of the determined mean track areas for the experiment with the C target at 158 GeV/nucleon after all corrections is shown in Fig. 2. One can see that for all fragments with charges $6 \leqslant Z \leqslant 82$, corresponding charge peaks can be found. Charge identification can be performed by counting charge numbers downward beginning with the beam peak. We finally achieve a charge resolution of $0.15e$, $0.5e$, and $1.0e$ for a single etch cone of charge $Z=6$, 26, and 82 for the experiments at 10.6 and 158 GeV/nucleon. For the experiment at 1.0 GeV/nucleon, however, individual charge peaks can only be resolved for $Z \leqslant 60$. For charges with $Z > 60$ we use the area difference between successive charge peaks measured for the experiments at the higher projectile energies to estimate the calibration. Therefore systematic errors for the charge calibration of $1.5e$ cannot be excluded for the experiments at 1.0 GeV/nucleon for charges with $Z > 60$.

III. INCLUSIVE CHARGE YIELDS

In Figs. 3–5 the measured inclusive charge yields for the experiments with different targets for each beam energy are shown. These results are not corrected for the fragmentation of projectile fragments produced in the targets. So the results at large and small charge numbers in particular may have systematic errors of up to 10%. For the experiments with the ^{208}Pb projectiles the yields for charges with $7 \leqslant Z \leqslant 79$ and for the experiments with the ^{197}Au projectiles the yields for charges with $7 \leqslant Z \leqslant 76$ are presented. Furthermore, we have analyzed reactions of projectiles with the detector materials CR-39($C_{12}H_{18}O_7$) and BP-1 (the composition is given in

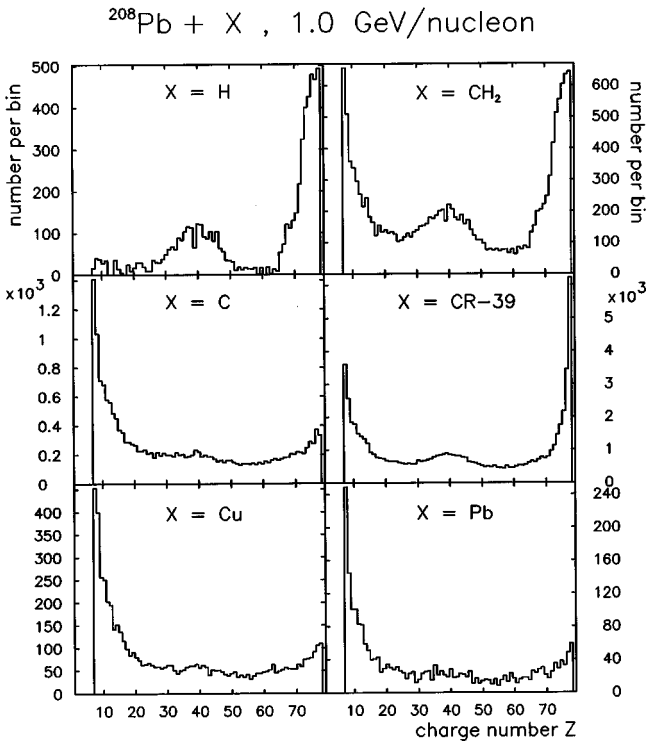

FIG. 3. Yield spectra for the charges of fragments measured for reactions of ^{208}Pb projectiles with H, CH_2, C, CR-39, Cu, and Pb at a beam energy of 1.0 GeV/nucleon.

[20]). The probability of a reinteraction of the projectile fragments produced is comparatively small for these materials because the detectors are thin in comparison to the targets mounted in stacks.

The spectra show significant target and energy dependences. The results for reactions of the projectiles with H can be extracted from the data for the C and CH_2 targets based on a statistical subtraction method. The spectrum of fragments produced in collisions of ^{208}Pb projectiles with H target nuclei at 1.0 GeV/nucleon (upper left part of Fig. 3) shows a peak around charge $Z=40$. This peak is caused by fission events. In addition to this peak only a few events can be found in the charge range $7 \leqslant Z \leqslant 65$. These few events may be generated by fragmentation of larger projectile fragments in the thick C and CH_2 targets or may be artifacts caused by the statistical subtraction method. For charges $Z > 65$ a steep increase of the yield with increasing Z is observed. One can conclude that at 1.0 GeV/nucleon the excitation energy of the projectile residues produced is not large enough to generate multifragmentation events for reactions of ^{208}Pb projectiles with H.

The spectra for reactions of ^{208}Pb projectiles with the heavier targets C, Cu, and Pb at 1.0 GeV/nucleon, however, show a comparable shape. In these reactions fragments with all possible charges are produced. Here one observes an increase of the charge yields with decreasing charge number for $Z \leqslant 20$. On the other hand, comparatively fewer fission and spallation events can be found. Therefore one can conclude that a wider excitation energy spectrum of the projectile residues produced can be explored in reactions with the

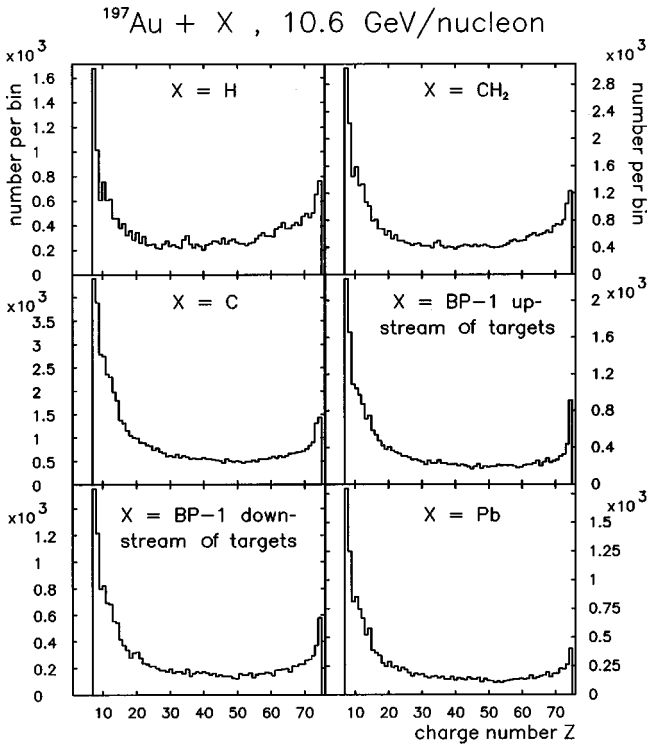

FIG. 4. Yield spectra for the charges of fragments measured for reactions of ^{197}Au projectiles with H, CH_2, C, BP-1 (up- and downstream of the targets), and Pb at a beam energy of 10.6 GeV/nucleon.

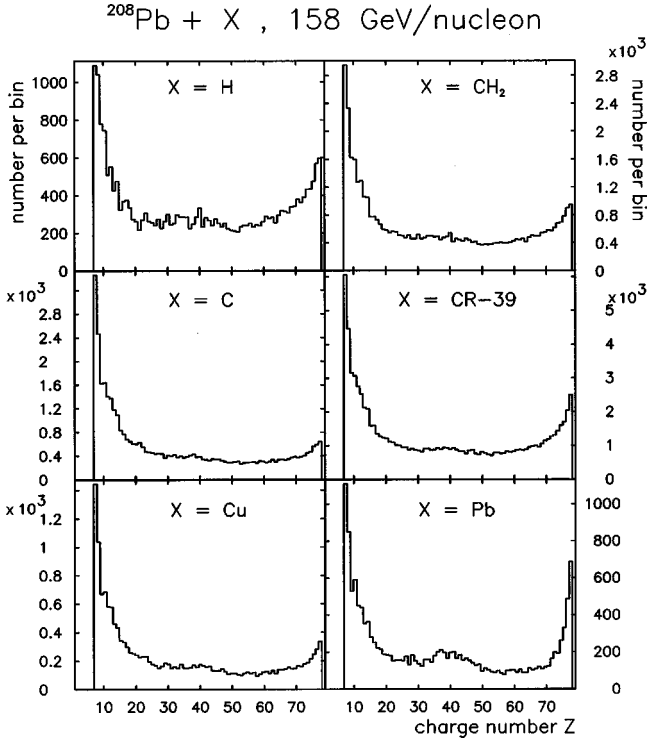

FIG. 5. Yield spectra for the charges of fragments measured for reactions of ^{208}Pb projectiles with H, CH_2, C, CR-39, Cu, and Pb at a beam energy of 158 GeV/nucleon.

heavier targets. At higher excitation energies the prefragments break up in multifragmentation. The spectra for interactions of the ^{208}Pb projectiles with CH_2 and CR-39 are a superposition of the spectra for reactions with the H, C, and O components.

The spectra for the reactions at the higher projectile energies show only a weak target dependence. Here the spectra for reactions with the H component differ less significantly from the spectra for the heavier targets than at 1.0 GeV/nucleon. One has to conclude that at the higher projectile energy the maximum possible excitation energy of the projectile residues is significantly enlarged for reactions of ^{208}Pb or ^{197}Au projectiles with H target nuclei. For the heavier targets significant energy dependences can be observed only for spallation and fission reactions. One finds especially for reactions of ^{208}Pb projectiles with a Pb target an increasing proportion of spallation and fission reactions at 158 GeV/nucleon. This energy dependence is caused by the electromagnetic dissociation process as described by Hirzebruch *et al.* [21]. Apart from this special fragmentation process, no significant target and energy dependences can be found for reactions of ^{208}Pb and ^{197}Au projectiles with a C, Cu, or Pb target. The observed independence of the shape for the elemental yields of the projectile energy is in agreement with the results of other experiments [22,23].

Furthermore, in Fig. 4 the spectra for reactions of ^{197}Au projectiles with the BP-1 detectors up- and downstream from the targets are plotted. For both cases the fragments were, identified only with the detectors downstream of the targets. Therefore the comparison of these spectra allows us to estimate the experimental bias caused by reinteractions of projectile fragments in the thick targets. These spectra show only small differences for the largest and smallest charge numbers.

IV. CHARGE CORRELATIONS

It is possible to study characteristics of fragmentation processes like fission or spallation based on inclusive charge yields of fragments. For the multifragmentation process, however, where several fragments are produced in the same interaction, these yield spectra give only limited information. Details about the reaction conditions like the size of the original projectile spectator are needed. For this purpose one uses the quantity Z_{bound} [7]. Z_{bound} is defined as the sum of the charges of all fragments with $Z \geqslant 2$ produced in the same interaction. Z_{bound} is closely related to the impact parameter and to the size of the original projectile spectator, as can be concluded from a simple geometric picture of the reaction process. Furthermore, it has been shown that Z_{bound} has a relation to the excitation energy per nucleon of the decaying prefragment [4].

Due to the detection threshold of the CR-39 foils we cannot determine Z_{bound} for the individual fragmentation events. Instead of this we use Z_{bound6} or Z_{bound7}. These quantities are defined as the sums of the charges of all particles with $Z \geqslant 6$ or $Z \geqslant 7$ produced in the same interaction. The dependence of the characteristics of multifragmentation on Z_{bound} and on Z_{bound6} or Z_{bound7} cannot be compared directly. It is

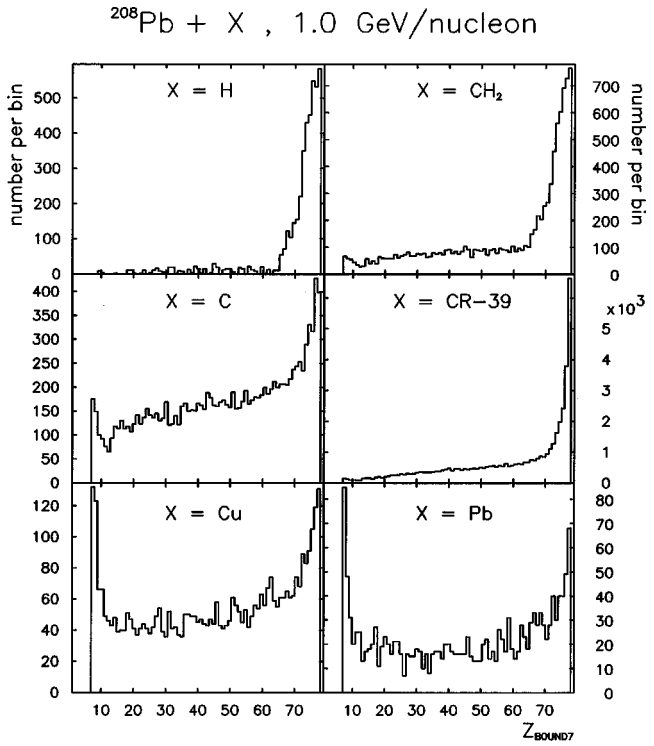

FIG. 6. Yield spectra for the charge sum Z_{bound7} measured for reactions of ^{208}Pb projectiles with H, CH_2, C, CR-39, Cu, and Pb at a beam energy of 1.0 GeV/nucleon.

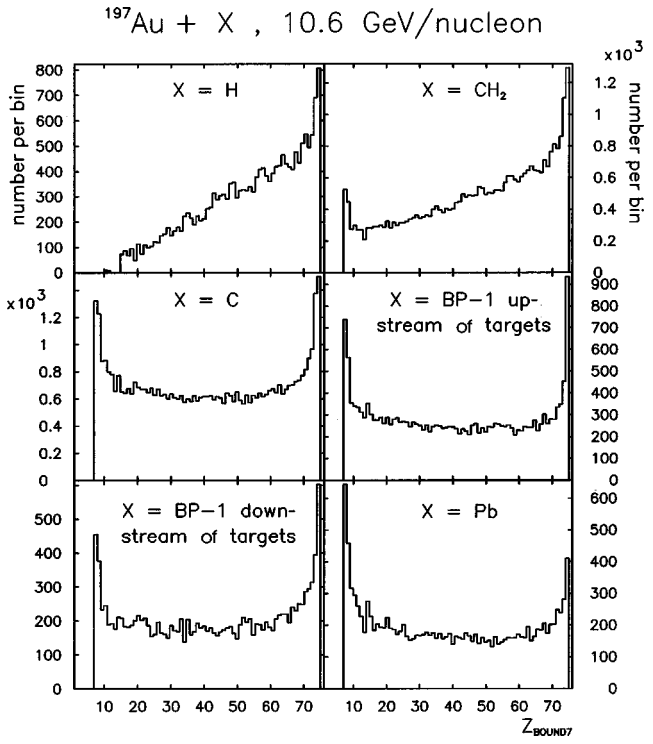

FIG. 7. Yield spectra for the charge sum Z_{bound7} measured for reactions of ^{197}Au projectiles with H, CH_2, C, BP-1 (up- and down-stream of the targets), and Pb at a beam energy of 10.6 GeV/nucleon.

evident that due to the loss of the information provided by the lighter fragments estimation of the impact parameter based on Z_{bound6} is less accurate than using Z_{bound}. However, the observed distributions for the Z_{bound7} values are strongly related to the distribution of the sizes of projectile spectators produced. Small Z_{bound7} values correspond to small projectile spectators and small impact parameters whereas large Z_{bound7} values correspond to large projectile spectators and large impact parameters.

In Figs. 6–8 the measured yield spectra for Z_{bound7} are plotted for experiments with ^{208}Pb projectiles at 1.0 GeV/nucleon, with ^{197}Au projectiles at 10.6 GeV/nucleon, and with ^{208}Pb projectiles at 158 GeV/nucleon in reactions with targets ranging from CH_2 to Pb. As for the inclusive charge yield spectra, significant target and energy dependences can be found. At 1.0 GeV/nucleon a strong target dependence for reactions with H, C, Cu, and Pb can be observed. For reactions with the H component only a few events with $Z_{\text{bound7}} \leqslant 65$ can be found. As for the charge yield spectra, one has to state that these events are probably caused by the reinteraction of projectile fragments in the thick targets, or are artificially generated by the statistical subtraction method applied for the H target. For $Z_{\text{bound7}} > 65$, however, a steep increase of the yields with increasing Z_{bound7} values can be recognized. One must conclude that the deposited excitation energy for reactions of ^{208}Pb projectiles with H is not sufficient at 1.0 GeV/nucleon to generate projectile residues with small charge numbers.

For reaction with the heavier targets C, Cu, and Pb, however, events are observed for all Z_{bound7} values. Nevertheless,

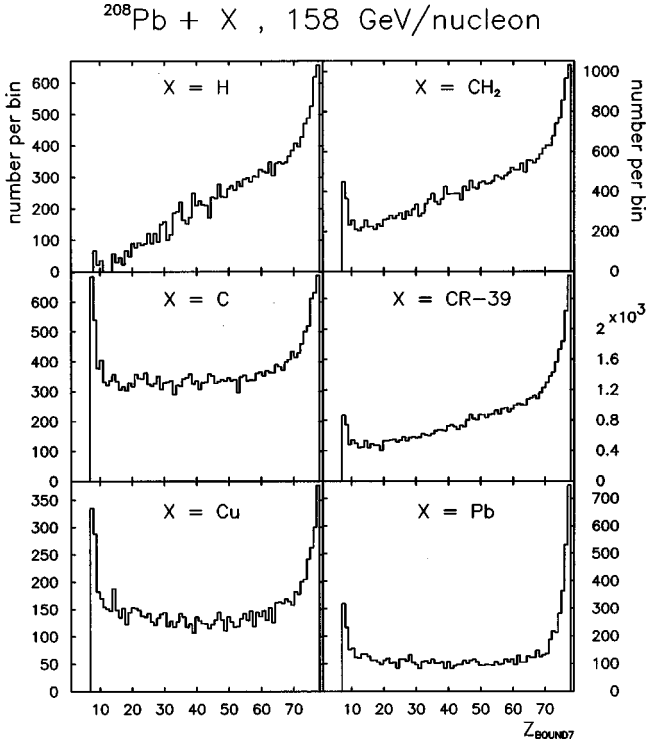

FIG. 8. Yield spectra for the charge sum Z_{bound7} measured for reactions of ^{208}Pb projectiles with H, CH_2, C, CR-39, Cu, and Pb at a beam energy of 158 GeV/nucleon.

comparison of the spectra for the C target with the spectra for the heavier targets shows a significant target dependence for the smaller Z_{bound7} values. For the C target comparatively few events with small Z_{bound7} values can be observed, in comparison to those for the Cu and Pb targets.

In the spectra for reactions of ^{197}Au and ^{208}Pb projectiles at 10.6 and 158 GeV/nucleon for collisions with C, BP-1, Cu, and Pb nuclei, no significant target dependence can be observed for $Z_{\text{bound7}} < 70$. For larger Z_{bound7} values a significant target dependence can be observed especially at 158 GeV/nucleon, which is caused by contributions of the electromagnetic dissociation process. Only the spectra for the H target differ significantly from those for the heavier targets. In these spectra only a few events can be found for the smallest Z_{bound7} values. Again one has to state that these may be artificial. For $14 \leqslant Z_{\text{bound7}} \leqslant 70$ a smooth increase of the yield with growing Z_{bound7} is observed. For larger Z_{bound7} values the spectra show a steeper increase of the yields. The low probability of observing events with small Z_{bound7} values indicates that in the analyzed projectile energy range the deposited excitation energy for all reactions with H is not sufficient for almost complete disintegration of ^{197}Au and ^{208}Pb projectiles.

Of particular interest are projectile energy dependences for the same target. A significant projectile energy dependence can be observed for reactions with H and C for projectile energies at 1.0 and 10.6 GeV/nucleon. For these reactions one can expect that at a higher projectile energy for the same impact parameter a somewhat smaller projectile residue will be formed due to increased evaporation of nucleons. Thus a larger excitation energy is deposited and the yield for small values of Z_{bound7} is enhanced.

For the Cu and Pb targets, however, no significant projectile energy dependences can be found, neglecting the fission and spallation reactions caused by the electromagnetic dissociation. This is a hint that for reactions with Cu and Pb targets in the energy range explored the fragmentation is governed only by the collision geometry. That means that the overlapping parts of the nuclei are abraded and form a fireball. The other part of the projectile is comparatively less excited and possesses almost the velocity of the incoming projectile. The spectra for the reactions with H and C for the experiments at 10.6 and 158 GeV/nucleon are almost identical. So one can infer that reactions of ^{197}Au and ^{208}Pb projectiles with H and C are controlled by the collision geometry of the processes for projectile energies above 10 GeV/nucleon. These observations indicate that it is not possible to disintegrate ^{197}Au and ^{208}Pb ions completely in reactions with H at projectile energies below 158 GeV/nucleon. One can expect furthermore that this conclusion will hold even for considerably higher projectile energies.

To study more details of the multifragmentation process we have used the quantity M_{IMF} and five variables describing charge correlations. M_{IMF} is the number of intermediate mass fragments produced in the same interaction. As in earlier experiments with Au projectiles, we define intermediate mass fragments as fragments with charges $3 \leqslant Z \leqslant 30$. But one has to keep in mind that only fragments with $Z \geqslant 6$ can be detected with CR-39 foils.

For investigation of the charge number of the heaviest fragment Z_{max} (also called Z_1) produced in the individual interactions, the quantity $Z_{\text{bound7}} - Z_{\text{max}}$ is used. The differences between the sizes of the heaviest, second heaviest, and third heaviest fragments Z_{max}, Z_2, and Z_3 produced in the same interaction event are explored with the charge asymmetries a_{12}, a_{23}, and a_{123}. a_{12} is defined as

$$a_{12} = \frac{Z_1 - Z_2}{Z_1 + Z_2}. \tag{1}$$

The charge correlation a_{23} is defined analogously to a_{12} but with Z_2 and Z_3. a_{123} is defined as

$$a_{123} = \frac{\sqrt{A_1^2 + A_2^2 + A_3^2}}{\sqrt{6}\langle Z \rangle}, \tag{2}$$

with

$$A_1 = Z_1 - \langle Z \rangle,$$

$$A_2 = Z_2 - \langle Z \rangle,$$

$$A_3 = Z_3 - \langle Z \rangle$$

$$\langle Z \rangle = \frac{Z_1 + Z_2 + Z_3}{3}.$$

Furthermore, we use the conditional moment γ_2 for investigation of the variance of the fragment size distribution produced in an event. The method of conditional moments has been suggested by Campi to investigate special aspects of fragmentation processes [24,25]. γ_2 is defined as

$$\gamma_2 = \frac{M_2 M_0}{M_1^2}. \tag{3}$$

The moments M_i are defined as

$$M_i = \sum_{j=1}^{n-1} Z_j^i, \tag{4}$$

where the sum is extended over all fragments produced in the same interaction except the largest one, which is considered as the percolating cluster. This quantity can be interpreted as the variance of the charge distribution for all fragments produced in the same interaction.

Results concerning the charge correlations for reactions of ^{208}Pb projectiles at 1.0 and 158 GeV/nucleon and of ^{197}Au projectiles at 10.6 GeV/nucleon with targets from CH_2 to Pb are presented in Figs. 9–11, where M_{IMF} and the five quantities defined above are shown in dependence on Z_{bound7}. In Fig. 9 the charge correlations for reactions of ^{208}Pb projectiles at 1.0 GeV/nucleon for the targets CH_2 (squares), C (circles), Cu (triangles), and Pb (diamonds) are shown. The data for the mean multiplicity $\langle M_{\text{IMF}} \rangle$ of intermediate mass fragments are presented in the upper left part of Fig. 9. First, no significant target dependences can be observed. For $7 \leqslant Z_{\text{bound7}} \leqslant 13$ the values are equal to $\langle M_{\text{IMF}} \rangle = 1.0$, due to

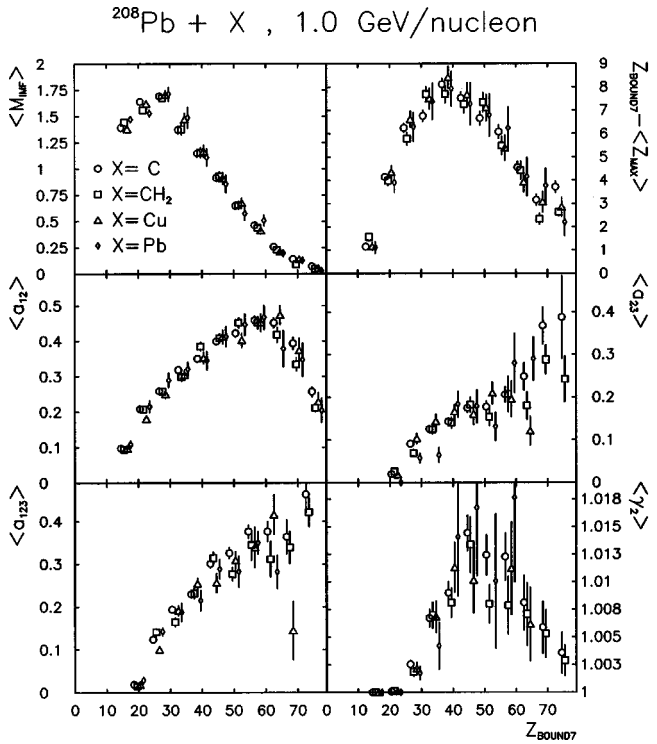

FIG. 9. The charge correlations $\langle M_{\mathrm{IMF}}\rangle$, $Z_{\mathrm{bound7}}-\langle Z_{\mathrm{max}}\rangle$, $\langle a_{12}\rangle$, $\langle a_{23}\rangle$, $\langle a_{123}\rangle$, and $\langle \gamma_2\rangle$ plotted versus Z_{bound7} for reactions of ^{208}Pb projectiles with C, CH_2, Cu, and Pb at a beam energy of 1.0 GeV/nucleon.

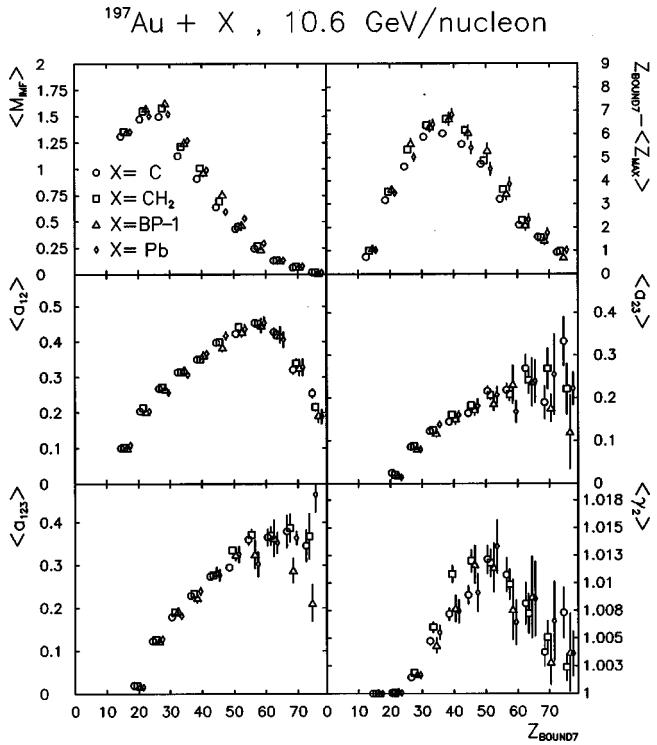

FIG. 10. The charge correlations $\langle M_{\mathrm{IMF}}\rangle$, $Z_{\mathrm{bound7}}-\langle Z_{\mathrm{max}}\rangle$, $\langle a_{12}\rangle$, $\langle a_{23}\rangle$, $\langle a_{123}\rangle$, and $\langle \gamma_2\rangle$ plotted versus Z_{bound7} for reactions of ^{197}Au projectiles with C, CH_2, BP-1, and Pb at a beam energy of 10.6 GeV/nucleon.

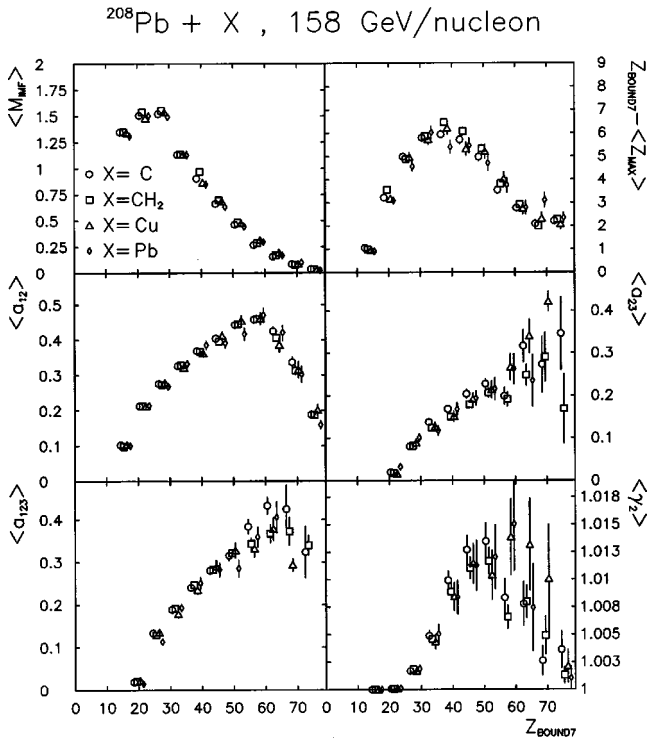

FIG. 11. The charge correlations $\langle M_{\mathrm{IMF}}\rangle$, $Z_{\mathrm{bound7}}-\langle Z_{\mathrm{max}}\rangle$, $\langle a_{12}\rangle$, $\langle a_{23}\rangle$, $\langle a_{123}\rangle$, and $\langle \gamma_2\rangle$ plotted versus Z_{bound7} for reactions of ^{208}Pb projectiles with C, CH_2, Cu, and Pb at a beam energy of 158 GeV/nucleon.

the detection threshold. For $14\leqslant Z_{\mathrm{bound7}}\leqslant 30$ an increase of the data with increasing Z_{bound7} can be found. At $Z_{\mathrm{bound7}}=30$ a rapid decrease of $\langle M_{\mathrm{IMF}}\rangle$ is observed, which is a result of the definition of intermediate mass fragments. Fragments with $Z\leqslant 30$ are counted with a multiplicity number 1 but fragments with $Z>30$ are excluded. For larger Z_{bound7} values a monotonic decrease down to values of almost 0 is found.

The quantity $Z_{\mathrm{bound7}}-\langle Z_1\rangle$ is plotted in the upper right part of Fig. 9. Again no significant target dependence can be observed. In the case of only one detected fragment in the reaction is the quantity $Z_{\mathrm{bound7}}-\langle Z_1\rangle$ equal to 0 for $7\leqslant Z_{\mathrm{bound7}}\leqslant 13$. For $14\leqslant Z_{\mathrm{bound7}}<40$ a steep increase with growing Z_{bound7} can be seen. For larger Z_{bound7} values the data show a rapid decrease.

In the middle left part of Fig. 9 the charge difference between the largest and second largest fragment is analyzed using the mean charge asymmetry $\langle a_{12}\rangle$. The plot shows a monotonic increase of the data with Z_{bound7} for $14\leqslant Z_{\mathrm{bound7}}\leqslant 55$. For larger Z_{bound7} values the shape of the data points shows a rapid decrease. Small values for $\langle a_{12}\rangle$ indicate that the largest fragment has a similar size to the second largest fragment. Large values around 1, however, reveal that the largest fragment is much larger than the second largest. So one has to conclude from the data that the size of the heaviest fragment in particular increases with growing Z_{bound7}. The decrease of $\langle a_{12}\rangle$ for $Z_{\mathrm{bound7}}>55$ is caused by fission events where two large fragments with almost the same size are produced. If one excludes the fission events from the presentation $\langle a_{12}\rangle$ rises for $Z_{\mathrm{bound7}}>55$ also.

In the middle right part of Fig. 9 events with three de-

tected fragments are explored. The charge asymmetry $\langle a_{23} \rangle$, analogous to $\langle a_{12} \rangle$, is used to investigate the size difference between the second and third largest fragments. As for $\langle a_{12} \rangle$, one observes an increase of $\langle a_{23} \rangle$ with increasing Z_{bound7} for $Z_{\text{bound7}} \geqslant 21$. Again one has to conclude that the size of the second heaviest fragment grows faster with Z_{bound7} than that of the third heaviest. Furthermore, the comparison between $\langle a_{12} \rangle$ and $\langle a_{23} \rangle$ exhibits a steeper increase for $\langle a_{12} \rangle$, which shows that the size difference between the largest and second largest fragments grows faster with Z_{bound7} than does the size difference between the second and third largest fragments.

The three-body asymmetry $\langle a_{123} \rangle$ shown in the lower left part of Fig. 9 investigates the size differences between the three largest fragments produced in the same interaction. Small values near 0 signal that the three fragments have a similar size. Values of about $\langle a_{123} \rangle = 0.3$ at $Z_{\text{bound7}} = 60$ represent events with two equal sized and one small fragment. A value of about $\langle a_{123} \rangle = 0.6$ at $Z_{\text{bound7}} = 60$ indicates one large and two small fragments produced in the reaction. Therefore one can conclude from the data that typically one large, one somewhat smaller, and one small fragment are produced for large Z_{bound7}.

As for $\langle M_{\text{IMF}} \rangle$ and $Z_{\text{bound7}} - \langle Z_1 \rangle$, the charge asymmetries $\langle a_{12} \rangle$, $\langle a_{23} \rangle$, and $\langle a_{123} \rangle$ show no significant target dependence. This target independence is confirmed within the experimental errors for the investigation of the mean conditional moment $\langle \gamma_2 \rangle$. As for $Z_{\text{bound7}} - \langle Z_1 \rangle$, the data for the smaller Z_{bound7} values show an increase of $\langle \gamma_2 \rangle$ and then a decrease with growing Z_{bound7}. For this charge correlation the maximum is located at $Z_{\text{bound7}} = 45$. That means that the variance of the charge distribution for the measured fragments produced in the same event is largest at $Z_{\text{bound7}} = 45$.

It should be stated that in general the data for the charge correlations are strongly influenced by autocorrelations, especially for the smaller Z_{bound7} values due to the small number of possible charge combinations. For example, the three-body asymmetry $\langle a_{123} \rangle$ has to be equal to 0 for $Z_{\text{bound7}} = 21$ because only events with three fragments with $Z = 7$ can contribute there. For the larger Z_{bound7} values, however, many charge combinations can contribute to the different Z_{bound7} channels. But one has to consider, for example, that the location of the measured maxima of the correlations may be influenced by strong autocorrelations. Thus one has to be careful with the interpretation of these results.

It is remarkable that the data show no significant target dependence for all analyzed charge correlations. Similar results were also found in experiments with electronic detector systems at energies from 0.4 to 1 GeV/nucleon considering only fragments with charges $Z \geqslant 6$ [9]. On the other hand, the new results are in contradiction to the results of an earlier experiment performed in our group [15], where a target dependence for $\langle M_{\text{IMF}} \rangle$ as a function of Z_{bound6} was observed. This dependence was artificially produced by systematic effects. The results for the H target were affected by uncertainties of the subtraction method and for the C and Pb target the results were affected by problems of the vertex reconstruction.

In Fig. 10 the charge correlations are investigated for reactions of ^{197}Au projectiles with targets of CH_2, C, BP-1, and Pb at 10.6 GeV/nucleon. One can observe that the shape of the data for all six charge correlations investigated resembles the measurements for the experiments at 1.0 GeV/nucleon. Significant target dependences can be observed only when comparing the data for the C target with the data for the other targets for the observables $\langle M_{\text{IMF}} \rangle$ and $Z_{\text{bound7}} - \langle Z_1 \rangle$. This target dependence is caused by the somewhat higher detection threshold for this special experiment with the C target. Therefore not all fragments with $Z = 7$ could be measured. This can also be seen in Fig. 4. There the ratio between the yield for charge $Z = 7$ and the yields for the larger charges $Z = 8$, 9, and 10 is significantly smaller in the spectrum for the C target than in the spectra for the other targets. One can estimate that only about 75% of the particles produced with charge $Z = 7$ could be measured in the experiment with the C target. Considering this fact, no significant target dependence can be found for the experiments performed at 10.6 GeV/nucleon with ^{197}Au projectiles. This target independence was also observed in an experiment with ^{197}Au projectiles at 10.6 GeV/nucleon using emulsions as target and detector material, but with much larger statistical uncertainties [10].

In Fig. 11 the results are plotted for the charge correlations for reactions with ^{208}Pb projectiles with the targets CH_2, C, Cu, and Pb at 158 GeV/nucleon. Again the shape of the data points for M_{IMF} and the five analyzed charge correlations is similar to that observed for the experiments at the other beam energies. Again no significant target dependence can be found.

In general, one can state that for all explored beam energies and projectile-target combinations investigated, no significant influence on the breakup mechanism of the produced projectile spectators was observed, considering only fragments with charge numbers $Z \geqslant 7$. This indicates that at all analyzed projectile energies the memory in the special entrance channel is lost before the breakup of the excited projectile residues occurs. Furthermore, the similarity of the shape of the data points shows that the excitation energies deposited in the projectile residues depend only weakly on the projectile energy.

For a more detailed investigation of the projectile energy dependences we concentrate on two target materials. The results for reactions of ^{208}Pb projectiles with CR-39 at 1.0 GeV/nucleon, for reactions of ^{197}Au projectiles with CH_2 at 10.6 GeV/nucleon, and for reactions of ^{208}Pb projectiles with CR-39 at 158 GeV/nucleon are presented in Fig. 12. We choose these projectile-target combinations due to the comparatively small probability of reinteractions of the projectile fragments produced in the detector material and the small statistical and systematic errors. One can see that the data points for the charge correlations $\langle M_{\text{IMF}} \rangle$, $Z_{\text{bound7}} - \langle Z_1 \rangle$, and γ_2 show significant energy dependences. For the charge asymmetries a_{12}, a_{23}, and a_{123}, however, no significant energy dependences can be found. In the plot for the mean number of intermediate mass fragments $\langle M_{\text{IMF}} \rangle$, one can observe that the values for the experiments at 1.0 GeV/nucleon are larger for almost all Z_{bound7} values than for the experiments performed at higher beam energies. For the experiments at 1.0 GeV/nucleon the maximum reaches a value of

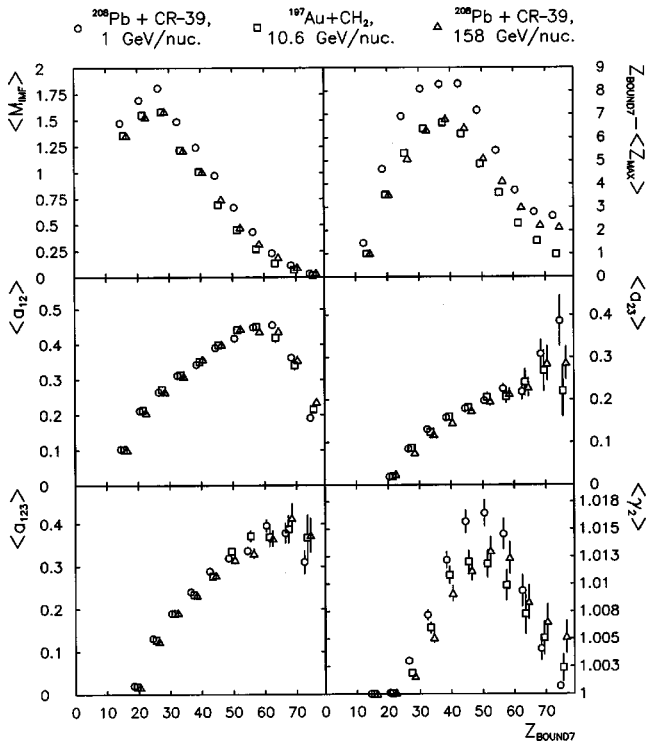

FIG. 12. The charge correlations $\langle M_{\mathrm{IMF}}\rangle$, $Z_{\mathrm{bound7}}-\langle Z_{\mathrm{max}}\rangle$, $\langle a_{12}\rangle$, $\langle a_{23}\rangle$, $\langle a_{123}\rangle$, and $\langle \gamma_2\rangle$ plotted versus Z_{bound7} for reactions of ^{208}Pb projectiles with CR-39 at 1.0 GeV/nucleon, for reactions of ^{197}Au projectiles with CH_2 at 10.6 GeV/nucleon, and for reactions of ^{208}Pb projectiles with CR-39 at 158 GeV/nucleon.

about $\langle M_{\mathrm{IMF}}\rangle = 1.8$ at $Z_{\mathrm{bound7}} = 30$. For the experiments at 10.6 and 158 GeV/nucleon one gets a maximum value of about $\langle M_{\mathrm{IMF}}\rangle = 1.6$. Analogous to $\langle M_{\mathrm{IMF}}\rangle$ the quantity $Z_{\mathrm{bound7}}-\langle Z_1\rangle$ exhibits a similar projectile energy dependence. Again the values for the experiments at 1.0 GeV/nucleon are above the values for the other beam energies. One finds maximum values of $Z_{\mathrm{bound7}}-\langle Z_1\rangle = 8.5$ for the experiments at 1.0 GeV/nucleon and maximum values of $Z_{\mathrm{bound7}}-\langle Z_1\rangle = 6.5$ for the experiments at 10.6 and 158 GeV/nucleon at $Z_{\mathrm{bound7}} = 40$. For $\langle \gamma_2\rangle$ also a significant projectile energy dependence can be observed. As observed for $\langle M_{\mathrm{IMF}}\rangle$ and $Z_{\mathrm{bound7}}-\langle Z_1\rangle$, the data points for the experiments at 1.0 GeV/nucleon are above those for the experiments at higher projectile energy for all Z_{bound7} values. One observes a maximum value of about $\langle \gamma_2\rangle = 1.016$ for the experiments at 1.0 GeV/nucleon and a maximum value of about $\langle \gamma_2\rangle = 1.013$ for the other projectile energies at $Z_{\mathrm{bound7}} = 50$.

The data points for the experiments at 10.6 and 158 GeV/nucleon, however, are almost identical for all six analyzed observables. Significant deviations can be observed only for $Z_{\mathrm{bound7}}-\langle Z_1\rangle$ and for $\langle \gamma_2\rangle$ for $Z_{\mathrm{bound7}} \geqslant 55$. These deviations can be attributed to different contributions by fission events. Apart from these deviations the agreement of the data points for both beam energies is remarkable. But one has to consider that the ^{197}Au projectiles used at 10.6 GeV/nucleon are about 5% smaller than the ^{208}Pb projectiles used for the experiments at 158 GeV/nucleon. So one can expect that the values for $\langle M_{\mathrm{IMF}}\rangle$, $Z_{\mathrm{bound7}}-\langle Z_1\rangle$, and $\langle \gamma_2\rangle$ will be somewhat larger for the experiments at 10.6 GeV/nucleon if one uses ^{208}Pb instead of ^{197}Au projectiles. Altogether, one can conclude that a weak but significant projectile energy dependence can be observed for the charge correlations $\langle M_{\mathrm{IMF}}\rangle$, $Z_{\mathrm{bound7}}-\langle Z_1\rangle$, and $\langle \gamma_2\rangle$ for heavy projectiles like ^{197}Au and ^{208}Pb in the energy range from 1 to 158 GeV/nucleon. The observation of a weak projectile energy dependence, especially of $\langle M_{\mathrm{IMF}}\rangle$ versus Z_{bound7}, is in qualitative agreement with the results of experiments performed with emulsions and electronic detector systems [10,11,13,12].

The observed projectile energy dependence can be understood if the excitation energy of the prefragments is somewhat smaller at the higher projectile energy. A reduced probability for the breakup of the prefragments into more than one detectable fragment would originate from smaller excitation energies. This is indicated by the fact that the mean size of the heaviest fragment is somewhat larger at the higher beam energy than for the smaller ones. The multiplicity distribution $\langle M_{\mathrm{IMF}}\rangle$ of intermediate mass fragments confirms this interpretation. This quantity shows that at the higher beam energy fewer intermediate mass fragments are produced than at the lower energy, indicating also a reduced probability for the breakup of the prefragments into several smaller particles.

For the charge asymmetries $\langle a_{12}\rangle$, $\langle a_{23}\rangle$, and $\langle a_{123}\rangle$, however, where only some special fragmentation processes with two or three detected fragments are investigated, no significant projectile energy dependence can be found. From this independence one can infer that the breakup of the prefragment is a statistical process: depending on the excitation energy of the prefragment it decays statistically into more or fewer intermediate mass fragments.

The conclusion that the deposited excitation energy is somewhat smaller at the higher projectile energy can be understood based on the different kinematics. At 1.0 GeV/nucleon particles of the fireball can be scattered and backscattered in the projectile residues, because these have a velocity of $\beta \leqslant 0.85$ which is significantly smaller than the speed of light. At 158 GeV/nucleon, however, the velocity of the projectile spectators is comparable to the speed of light ($\beta = 0.999\,98$). So the probability for scattering and backscattering of particles emerging from the fireball is very small. This consideration reveals that the assumption of smaller excitation energies of the projectile residues at the higher beam energies is quite reasonable. On the other hand, this weak projectile energy dependence shows that the contribution to the excitation energy of the projectile spectators by scattered and backscattered particles emerging from the fireball is also rather small at 1.0 GeV/nucleon.

In Fig. 13 the projectile energy dependence observed for the mean number of intermediate mass fragments $\langle M_{\mathrm{IMF}}\rangle$ is analyzed in more detail. In this figure the mean multiplicity $\langle N_{Z_n}+\cdots+N_{Z_m}\rangle$ of fragments with charges $7 \leqslant Z \leqslant 8$, $9 \leqslant Z \leqslant 12$, $13 \leqslant Z \leqslant 16$, $17 \leqslant Z \leqslant 20$, $21 \leqslant Z \leqslant 24$, and $25 \leqslant Z \leqslant 28$ is presented. For all explored charge ranges a significant projectile energy dependence can be observed almost over the whole Z_{bound7} range. As for $\langle M_{\mathrm{IMF}}\rangle$, the values for the experiments at 1.0 GeV/nucleon are larger than those for the experiments at the higher projectile energies. The results for

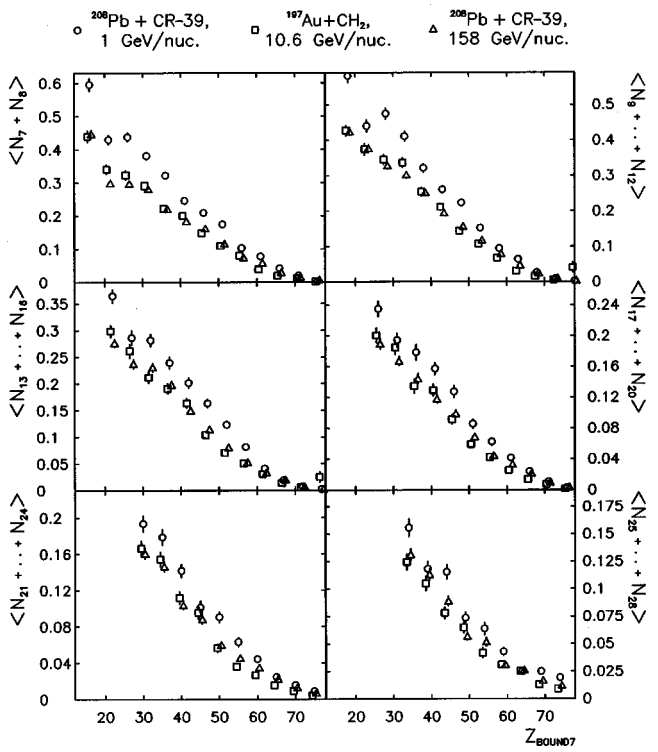

FIG. 13. The mean multiplicities $\langle N_{Z_n} + \ldots + N_{Z_m} \rangle$ for the charge ranges $7 \leqslant Z \leqslant 8$, $9 \leqslant Z \leqslant 12$, $13 \leqslant Z \leqslant 16$, $17 \leqslant Z \leqslant 20$, $21 \leqslant Z \leqslant 24$, and $25 \leqslant Z \leqslant 28$ plotted versus Z_{bound7} for reactions of ^{208}Pb projectiles with CR-39 at 1.0 GeV/nucleon, for reactions of ^{197}Au projectiles with CH_2 at 10.6 GeV/nucleon, and for reactions of ^{208}Pb projectiles with CR-39 at 158 GeV/nucleon.

the experiments at 10.6 and 158 GeV/nucleon are identical within the error bars. As stated before, this is due to the fact that the experiments at 10.6 GeV/nucleon were performed with ^{197}Au projectiles. Again one can assume that the values would be somewhat larger if one used ^{208}Pb instead of ^{197}Au projectiles for the experiments at 10.6 GeV/nucleon. Furthermore, one can observe that the projectile energy dependence is rather pronounced for fragments with small charge numbers at small Z_{bound7} values. Thus one can conclude that the observed projectile energy dependence holds for all intermediate mass fragments in almost the whole Z_{bound7}-range.

It should be mentioned that the observed weak projectile energy dependence is in qualitative agreement with the data taken with emulsions at projectile energies of 10.6 and 158 GeV/nucleon for heavy projectiles [10,11,13,12]. However, in these studies the number of analyzed fragmentation events is too small to detect small differences in the breakup processes, especially for the heavier intermediate mass fragments. Nonetheless, the data reveal significant projectile energy dependences, especially for the multiplicity distributions of light intermediate mass fragments, if one compares these data with those, for example, of the ALADIN collaboration taken for reactions of ^{197}Au projectiles with different targets at around 1.0 GeV/nucleon [9].

V. CONCLUSION

In this paper we have studied target and energy dependences for the fragmentation processes of ^{208}Pb and ^{197}Au projectiles in reactions with targets from CH_2 to Pb in the projectile energy range from 1 to 158 GeV/nucleon using the nuclear track detectors CR-39 and BP-1. Fragments with charges $Z \geqslant 7$ were measured with high efficiency. The experiments were performed with high statistical significance.

For the yield spectra of the fragment charge Z and the charge sum Z_{bound7}, it was shown that significant target dependences can be observed at all three projectile energies. The shape of the data points for reactions with H especially deviates significantly from those for the other projectile-target combinations. This indicates that the accessible excitation energy of the projectile residues produced is much lower than for reactions with the heavier targets.

Furthermore, one can conclude from the results for the yield spectra that the reaction process is mainly governed by the collision geometry of the interaction for projectile energies $E_p \geqslant 10$ GeV/nucleon. This means that almost no projectile energy dependences can be observed in the yield spectra for projectile energies $E_p \geqslant 10$ GeV/nucleon.

Some aspects of multifragmentation processes of heavy projectiles were investigated based on charge correlations. It can be stated that for all of these six charge observables no significant target dependences can be found at 1.0, 10.6, and 158 GeV/nucleon. One can conclude that the memory in the special entrance channel of the reaction is lost before the excited prefragments break up into smaller particles, possibly from an equilibrated state.

The analysis of the projectile energy dependence reveals that for charge correlations where all interactions are considered a weak but significant projectile energy dependence is observed. However, for the charge asymmetries where only reactions with two and more detected fragments are explored, no significant projectile energy dependence can be found. From this observation one can infer that a prefragment with a certain excitation energy will always break up in the same manner. This is a further hint for a breakup from an equilibrated state. Thus one can conclude that the observed projectile energy dependence is caused by a rarer breakup of the prefragments into smaller pieces at the higher projectile energies, which may be a hint for somewhat smaller mean excitation energies of the projectile residues at the higher projectile energies. The assumption of somewhat smaller excitation energies at the higher projectile energies seems to be reasonable, if one considers the kinematics of the reactions. At smaller projectile energies the probability for the scattering of fireball particles into the projectile residues is larger than at the higher projectile energies. Furthermore, one can conclude that the contribution of backscattered particles emerging from the fireball is rather small for all projectile energies.

ACKNOWLEDGMENTS

We thank the staff of the GSI/SIS, of the BNL/AGS, and of the CERN/SPS for excellent support during the exposures. This work was funded by the BMBF under Contract No. 06SI3673.

[1] H. Jaqaman, A. Mekjian, and L. Zamick, Phys. Rev. C **27**, 2782 (1983).
[2] A. Panagiotou, M. Curtin, H. Toki, D. Scott, and P. Siemens, Phys. Rev. Lett. **52**, 496 (1984).
[3] N. Porile *et al.*, Nucl. Phys. **A471**, 149c (1987).
[4] J. Pochodzalla *et al.*, Phys. Rev. Lett. **75**, 1040 (1995).
[5] C. Ogilvie *et al.*, Phys. Rev. Lett. **67**, 1214 (1991).
[6] J. Hubele *et al.*, Z. Phys. A **340**, 263 (1991).
[7] J. Hubele *et al.*, Phys. Rev. C **46**, 1577 (1992).
[8] P. Kreutz *et al.*, Nucl. Phys. **A556**, 672 (1993).
[9] A. Schüttauf *et al.*, Nucl. Phys. **A607**, 457 (1996).
[10] P. Jain, G. Singh, and A. Mukhopadhyay, Phys. Rev. C **50**, 1085 (1994).
[11] M. Cherry *et al.*, Phys. Rev. C **52**, 2652 (1995).
[12] G. Singh and P. Jain, Phys. Rev. C **54**, 3185 (1996).
[13] M. Adamovich *et al.*, Z. Phys. A **359**, 277 (1997).
[14] J. Dreute, W. Heinrich, G. Rusch, and B. Wiegel, Phys. Rev. C **44**, 1057 (1991).
[15] G. Rusch, W. Heinrich, B. Wiegel, E. Winkel, and J. Dreute, Phys. Rev. C **49**, 901 (1994).
[16] W. Trakowski, B. Schöfer, J. Dreute, S. Sonntag, J. Beer, C. Brechtmann, H. Drechsel, and W. Heinrich, Nucl. Instrum. Methods Phys. Res. A **225**, 92 (1984).
[17] G. Rusch, E. Winkel, A. Noll, and W. Heinrich, Nucl. Tracks Radiat. Meas. **19**, 261 (1991).
[18] E. Benton, U. S. Naval Radiological Defense Laboratory Technical Report 68-14 (unpublished).
[19] W. Heinrich *et al.*, Radiat. Meas. **25**, 203 (1995).
[20] S. Wang, S. Barwick, P. Ifft, P. Price, and A. Westphal, Nucl. Instrum. Methods Phys. Res. B **35**, 43 (1988).
[21] S. Hirzebruch, E. Becker, G. Hüntrup, T. Streibel, E. Winkel, and W. Heinrich, Phys. Rev. C **51**, 2085 (1995).
[22] B. Berthier, R. Boisgard, J. Julien, J. Hisleur, R. Lucas, C. Mazur, C. Ngô, M. Ribrag, and C. Cerruti, Phys. Lett. B **193**, 417 (1987).
[23] W. Trautmann, U. Milkau, U. Lynen, and J. Pochodzalla, Z. Phys. A **344**, 447 (1993).
[24] X. Campi, J. Phys. A **19**, 917 (1986).
[25] X. Campi, Phys. Lett. B **208**, 351 (1988).